Quantum information processing using frequency control of impurity spins in diamond

A. M. Zagoskin,[1,2] J. R. Johansson,[2] S. Ashhab,[2] and Franco Nori[2,3]
[1]*Department of Physics and Astronomy, The University of British Columbia, Vancouver, British Columbia, Canada V6T 1Z1*
[2]*Digital Materials Laboratory, Frontier Research System, RIKEN, Wako-shi, Saitama 351-0198, Japan*
[3]*Center for Theoretical Physics, Physics Department and Center for the Study of Complex Systems, The University of Michigan, Ann Arbor, Michigan 48109-1040, USA*
(Received 7 March 2007; published 27 July 2007)

Spin degrees of freedom of charged nitrogen-vacancy (NV^-) centers in diamond have large decoherence times even at room temperature, can be initialized and read out using optical fields, and are therefore a promising candidate for solid-state qubits. Recently, quantum manipulations of NV^- centers using rf fields were experimentally realized. In this paper, we provide a theoretical demonstration, first, that such operations can be controlled by varying the frequency of the signal, instead of its amplitude, and NV^- centers can be selectively addressed even with spacially uniform rf signals; second, that when several NV^- centers are placed in an off-resonance optical cavity, a similar application of classical optical fields provides a controlled coupling and enables a universal two-qubit gate (CPHASE). rf and optical control together promise a scalable quantum computing architecture.

DOI: 10.1103/PhysRevB.76.014122 PACS number(s): 78.67.−n, 03.67.Lx, 76.30.Mi

I. INTRODUCTION

Impurity spins in diamond are among the most promising candidates for solid-state quantum hardware. The so-called (negatively charged) nitrogen-vacancy (NV^-) centers have a low-lying spin triplet state $^3A_2$ with a large decoherence time (up to $\sim 350\ \mu$s) at room temperature, which can be initialized and read out using a strong, spin-conserving optical transition to the excited ^3E state.[1–6] The coherent manipulation of the $^3A_2$ state and its coupling to spins of ^{13}C (Refs. 2 and 6) and N (Refs. 4 and 5) demonstrated the feasibility of NV^--based quantum devices. Though the direct coupling of different NV^- centers, necessary for a scalable architecture, would require placing them too close to each other (within a few nanometers), coupling through an optical mode is possible[7–9] using Stark shifts, in order to tune the coupling on and off. (Stark shifts in NV^- were observed in bulk response[10–12] as well as from individual centers.[13])

The use of local time-dependent fields for selective control is a natural approach, but it is not always easily achieved in the case of microscopic qubits. Here, we suggest an approach which would allow us to address specific NV^- centers by tuning to their resonant frequency, which can be made position dependent by the application of a *static* nonuniform magnetic field. We will also show that a similar approach using classical optical fields allows controlled coupling and universal two-qubit gates for NV^- centers in an optical cavity.

II. MODEL

A NV^- center is a negatively charged complex of a nitrogen impurity and a neighboring vacancy. It can be formed as a result of nitrogen implantation in the diamond matrix; in experiments so far, the conversion from N to NV^- was achieved with a limited efficiency of about 5%.[4] It is, therefore, common to find a NV^- center close to a nitrogen impurity. Unlike a NV^- center, a nitrogen impurity does not have an electric dipolar moment and does not couple to optical fields. Consider such a N-NV^- complex.[4,5] Let us choose the [111] direction as the z axis. The magnetic moment (spin 1) of the NV^- center and the eigenvalues of its z component are $\vec{S}$ and $M_z=0,\pm 1$. For the N impurity (spin 1/2), they are denoted respectively by $(1/2)\vec{\sigma}$ and $m_z=\pm 1/2$; $\vec{\sigma}$ is the vector of Pauli matrices. The $^3A_2$ ground state of the NV^- center is split by the crystal field, while the $(M_z=\pm 1)$ states are degenerate, and the $(M_z=0)$ state becomes the true ground state. The $(M_z=0)$ state leads to enhanced photoluminescence through the excitation to ^3E [states $M_z=\pm 1$ undergo frequent transitions to a metastable level ^1A, which is strictly forbidden for the $(M_z=0)$ state]; this allows an optical readout.[2–5] The external magnetic field along the z axis splits the $(M_z=\pm 1)$ states as well as the $(m_z=\pm 1/2)$ spin states of the nitrogen impurity. The Hamiltonian of the system is (in the absence of an electric field)

$$H = H_{NV} + H_N + H_{\text{int}}, \tag{1}$$

where

$$H_{NV} = D(S_z)^2 + \kappa \vec{B}\cdot\vec{S}, \tag{2}$$

$$H_N = \frac{1}{2}\kappa\vec{B}\cdot\vec{\sigma} + A\vec{\sigma}\cdot\vec{I}. \tag{3}$$

Here, $D=2.88$ GHz,[14–16] $\kappa=2.8$ MHz/Gs,[4,5] the hyperfine splitting $A=86$ or 114 MHz depending on the position of the nitrogen in the lattice,[17] and $\vec{I}$ is its nuclear spin $(I=1)$. The magnetic dipolar interaction

$$H_{\text{int}} = \gamma[\vec{S}\cdot\vec{\sigma} - 3(\vec{S}\cdot\vec{n})(\vec{\sigma}\cdot\vec{n})] \tag{4}$$

has a scale $\gamma \approx 6.5$ MHz for a distance of 2 nm between NV^- and N; $\vec{n}$ is the unit vector in the direction connecting N and NV^-.

When $B_z=B_{\text{res}}=514$ Gs (while $B_x=B_y=0$), the transition $(M_z=0)\leftrightarrow(M_z=-1)$ in the NV^- center is in resonance with

the transition $(m_z=+1/2)\leftrightarrow(m_z=-1/2)$ in N. The term (4) then induces coherent transitions in the system, which were experimentally observed in Refs. 4 and 5. Other resonances, shifted by $\sim$15 Gs to either side due to the hyperfine interaction in N, were also observed. (The hyperfine splitting in the NV^- center was too small to be resolved;[5] we neglect it here.)

In order to distinguish different NV^- centers, we now consider the application of a B_z field gradient. For example, if they are placed 10 μm apart, a field gradient of 1 T/cm will produce a 30 MHz difference in the $(M_z=0)\leftrightarrow(M_z=-1)$ transition frequency between the neighboring centers, which is enough for our purposes, as we shall see below.

III. rf CONTROL OF SINGLE-SPIN ROTATIONS IN NV^- CENTERS

If the field $B_z\neq B_{\mathrm{res}}$, the transitions

$$(M_z=0;m_z=1/2)\leftrightarrow(M_z=-1;m_z=-1/2)$$

are suppressed. (Note that these energy-conserving transitions do not conserve spin.) Single-qubit operations on a NV^- center can then be performed by applying a *spatially uniform* ac field along the y axis, with the resonance frequency $\omega_y=D-\kappa B_z$ (of order of 1.5 GHz) corresponding to the $(M_z=0)\leftrightarrow(M_z=-1)$ transitions:

$$H_y=\kappa B_y\cos\omega_y t\, S_y. \tag{5}$$

Due to the B_z gradient, this frequency is different for different NV^- centers, and we have *frequency-based* control. First, we go to the interaction representation:

$$H\rightarrow U_{NV}H\,U_{NV}^{\dagger}-iU_{NV}\frac{\partial}{\partial t}[U_{NV}^{\dagger}], \tag{6}$$

where

$$U_{NV}=\exp[iH_{NV}t]=(1-S_z^2)+(S_z^2\cos\kappa B_z t+iS_z\sin\kappa B_z t)\exp[iDt]. \tag{7}$$

Now we apply the rotating wave approximation (RWA), i.e., neglect the fast rotating terms with the frequencies $\sim D$, κB_z, $(D-\kappa B_z)$, ω_y compared to the slow terms with $\omega\sim(D-\kappa B_z)-\omega_y$. This is a commonly used trick (see, e.g., Ref. 18, Sec. 15.3.1), which is justified if the fast terms are averaged to zero when the equations of motion are integrated over a time short compared to the slow period, $2\pi/\omega$.

The resulting effective Hamiltonian

$$H_{y,\mathrm{eff}}=\frac{\kappa B_y}{2}\left[\frac{S_y-[S_z,S_y]_+}{\sqrt{2}}\right]\equiv\frac{\kappa B_y}{2}\sigma_y^{NV}. \tag{8}$$

The operator in brackets acts as the Pauli matrix σ_y on the subspace $\{M_z=0,\ M_z=-1\}$. The ac field produces relatively fast rotations of a chosen NV^- center, in excess of 1 MHz/G.

The use of frequency instead of amplitude rf control is not dictated solely by the fact that the latter would require a local (within a few microns) application of rf fields. The latter is feasible, though with the addition of extra circuits,[19] and, for somewhat bigger devices, is being done in experiments with superconducting flux and phase qubits on a regular basis (see, e.g., Ref. 20). The frequency control[21] will be certainly preferable when it is easier to produce sharp and precise changes in the frequency of the rf signal than in its amplitude.

IV. rf CONTROL OF NV^-–N COUPLING

A relatively weak ac field with appropriate frequency can turn on the transitions $(M_z=0;m_z=1/2)\leftrightarrow(M_z=-1;m_z=-1/2)$. To see this, we again perform a unitary transformation of the Hamiltonian to the interaction representation,

$$H\rightarrow U_N U_{NV}H\,U_{NV}^{\dagger}U_N^{\dagger}-iU_N U_{NV}\frac{\partial}{\partial t}[U_{NV}^{\dagger}U_N^{\dagger}], \tag{9}$$

where U_{NV} was defined in Eq. (7), and

$$U_N=\exp[iH_N t]=\cos[(\kappa B_z+AI_z)t/2]+i\sigma_z\sin[(\kappa B_z+AI_z)t/2]. \tag{10}$$

The resonance condition for the transition $(M_z=0;m_z=1/2)\leftrightarrow(M_z=-1;m_z=-1/2)$ is $2\kappa B_z+AI_z-D=0$. Assuming a detuning $\delta\omega$ from resonance, i.e.,

$$2\kappa B_z+AI_z-D=\delta\omega, \tag{11}$$

we find [from Eq. (9)] the effective interaction

$$H_{\mathrm{eff}}=\gamma(1-3n_z^2)S_z\sigma_z+\frac{\cos(\delta\omega\, t)}{2\sqrt{2}}\gamma(2-3n_x^2-3n_y^2)\times[\sigma_x^{NV}\sigma_x+\sigma_y^{NV}\sigma_y] \tag{12}$$

[with the same notation as in Eq. (8)]. The second term in the right-hand side of Eq. (12) is fast rotating and should be dropped in the RWA, unless the detuning $\delta\omega$ can be compensated. This is done by an additional field along the z axis, $B_z'(t)=\eta\kappa B_z\sin\omega t$. [The corresponding term in the Hamiltonian is not affected by the transformation (9).] After one more unitary transformation,

$$H_{\mathrm{eff}}\rightarrow U'H_{\mathrm{eff}}U'^{\dagger}-iU'\frac{\partial}{\partial t}[U'^{\dagger}], \tag{13}$$

with

$$U'=\exp\left[-i\eta\kappa B_z\left(S_z+\frac{1}{2}\sigma_z\right)\frac{\cos(\omega t)}{\omega}\right], \tag{14}$$

and assuming $\omega=\delta\omega$, we obtain, in the RWA, the following Hamiltonian:

$$\tilde{H}_{\mathrm{eff}}=\gamma(1-3n_z^2)S_z\sigma_z+\frac{J_1(2\eta\kappa B_z/\omega)}{2\sqrt{2}}\gamma(2-3n_x^2-3n_y^2)\times[\sigma_x^{NV}\sigma_x+\sigma_y^{NV}\sigma_y]. \tag{15}$$

Otherwise, the effective coupling is zero. Here, J_1 is a Bessel function.

The coupling strength, $\gamma\approx6.5$ MHz, determines how far we should be off-resonance in order to achieve decoupling. A

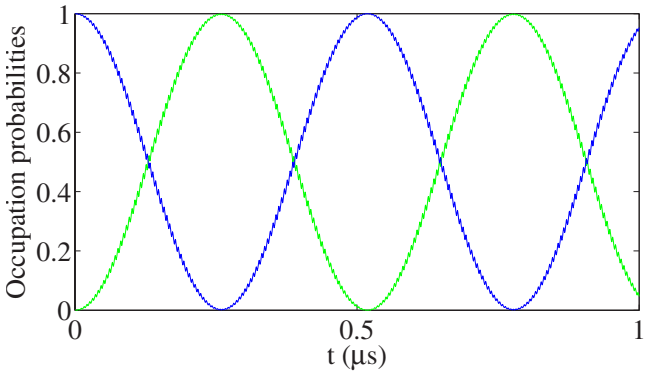

FIG. 1. (Color online) The occupation probabilities of the NV^- center ground state $M_z=0$ (light curve) and the excited state $M_z=-1$ (dark curve) as a function of time, for the NV^--N detuning $\delta\omega=0.2$ GHz and the ac field amplitude $\kappa B_z'=67$ MHz (corresponding to $\eta=0.05$, with static field amplitude $\kappa B_z=1.34$ GHz); $\gamma=6.5$ MHz. The transition frequency, ≈ 2 MHz, agrees with the RWA value following Eq. (15).

large detuning is also needed to justify the approximations leading to Eq. (15). The coupling is switched on by the ac field $B_z'(t)$. The coupling strength will be smaller than γ, but not drastically. Even choosing $\delta\omega=0.2$ GHz, $\eta=B_z'/B_{\text{res}}=0.05$, and remembering that $\kappa B_{\text{res}}\approx 1.5$ GHz, we find the attenuation of the coupling strength ≈ 0.32. It will still produce coherent transitions at ~ 2 MHz, which is fast compared to the decoherence times at room temperature of up to 0.35 ms.

Numerical simulations of the system described by the Hamiltonian in Eqs. (1)–(4) agree well with the predictions of the effective Hamiltonian [Eq. (15) and its generalization that can be derived following Ref. 22]. In the numerical simulations, the NV^- center was truncated to the subspace $\{M_z=0, M_z=-1\}$ and the external magnetic fields were chosen to be parallel to the z axis. This truncation is justified because the $M_z=1$ state of the NV^- center is very high in energy and is, therefore, not involved in the dynamics. Figure 1 shows the time evolution of the coupled NV^--N system as calculated from the time-dependent Schrödinger equation with the truncated Hamiltonian. Figure 2 shows the amplitude of the $|M_z=0, m_z=1/2\rangle \leftrightarrow |M_z=-1, m_z=-1/2\rangle$ oscillations, which represent a two-qubit operation, as a function of external-field driving frequency. These calculations confirm the validity of the RWAs leading to the effective Hamiltonian [Eq. (15)].

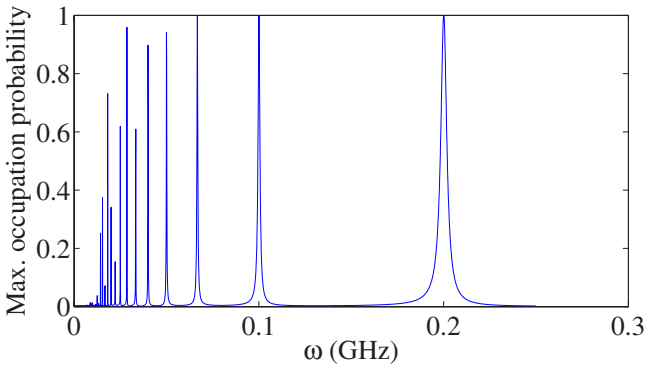

FIG. 2. (Color online) Maximum occupation probability for the NV^- center ground state, max ρ_{00}^{NV}, when initially in the excited state, as a function of the ac field frequency ω for the same choice of parameters as in Fig. 1. Note additional peaks at integral fractions of $\delta\omega$, which correspond to the higher-order (multiphoton) processes, dropped from Eq. (15). The higher-order peaks do not reach unit height because of limited frequency resolution and evolution time in the numerical simulation.

As an aside, in the same way, one can show that when the system is in resonance, an ac field $B_z'(t)$ will suppress the transitions and freeze the spins in NV^- and N (coherent destruction of tunneling; see, e.g., Ref. 22). This is not useful to the coupling scheme we are describing here.

In order to perform arbitrary one-qubit rotations of nitrogen spins, as well as two-qubit gates between NV^- and N, we only need to initialize NV^- and perform single-qubit rotations on it (see, e.g., Ref. 23 where the phase qubit is analogous to a NV^- center, and the quantum two-level system to a N impurity spin), which can be done using the rf control [Eq. (8)].

V. NV^-–NV^- AND INDIRECT N-N COUPLINGS

The scalability of the design requires the coupling between different NV^- centers or NV^--N complexes. For macroscopic qubits, this is done through the magnetic flux or charge coupling to cavity modes.[23–26] In our case, unfortunately, the magnetic coupling is way too weak. Instead, we can use an optical cavity mode and two classical laser fields, along the lines of Refs. 8 and 27. This has the disadvantage of involving the ^3E state, where the decoherence rate is higher. On the other hand, the laser fields are easier to apply locally. By tuning the frequency of the laser field, the interaction strength can be controlled.

Consider two NV^- centers placed in an off-resonance optical cavity. The Hamiltonian of the system is

$$H = H_0 + H_{\text{field}} + H_{\text{cavity}}, \tag{16}$$

$$H_0 = \omega_c a^\dagger a + \frac{E}{2}(I+\sigma_1^z) + \left(\frac{E+\Omega_1}{2}I + \frac{E-\Omega_1}{2}\tau_1^z\right) + \frac{E}{2}(I+\sigma_2^z) + \left(\frac{E+\Omega_2}{2}I + \frac{E-\Omega_2}{2}\tau_2^z\right), \tag{17}$$

$$\begin{aligned} H_{\text{field}} &= H_{\text{field},1} + H_{\text{field},2} \\ &= g_{1x}^{(0)}\mathcal{E}_1^{(0)}\cos(\omega_1^{(0)}t)\sigma_1^x + g_{1x}^{(-1)}\mathcal{E}_1^{(-1)}\cos(\omega_1^{(-1)}t)\tau_1^x \\ &\quad + g_{2x}^{(0)}\mathcal{E}_2^{(0)}\cos(\omega_2^{(0)}t)\sigma_2^x + g_{2x}^{(-1)}\mathcal{E}_2^{(-1)}\cos(\omega_2^{(-1)}t)\tau_2^x, \end{aligned} \tag{18}$$

$$\begin{aligned} H_{\text{cavity}} &= H_{\text{cavity},1} + H_{\text{cavity},2} \\ &= g_{1z}^{(0)}\epsilon(a^\dagger + a)\sigma_1^z + g_{1z}^{(-1)}\epsilon(a^\dagger + a)\tau_1^z + g_{2z}^{(0)}\epsilon(a^\dagger + a)\sigma_1^z \\ &\quad + g_{2z}^{(-1)}\epsilon(a^\dagger + a)\tau_2^z. \end{aligned} \tag{19}$$

Here, the operators

$$\sigma_j^z = |E_j\rangle\langle E_j| - |(A;M_z=0)_j\rangle\langle(A;M_z=0)0_j|,$$

$$\tau_j^z = |E_j\rangle\langle E_j| - |(A;M_z=-1)_j\rangle\langle(A;M_z=-1)_j|,$$

$$\sigma_j^x = |E_j\rangle\langle(A;M_z=0)_j| + |(A;M_z=0)_j\rangle\langle E_j|,$$

$$\tau_j^z = |E_j\rangle\langle(A;M_z=-1)_j| + |(A;M_z=-1)_j\rangle\langle E_j|$$

account for the optical transition ${}^3A \leftrightarrow {}^3E$ in the jth NV^- center. The term H_{field} describes the interaction of the electric moments of the NV^- centers with the classical laser fields, $\mathcal{E}_{1,2}^{(0,-1)}$, with frequencies $\omega_{1,2}^{(0,-1)}$, polarized in the x direction; H_{cavity} describes their interaction with the optical cavity mode polarized in the z direction, ϵ is the "electric field amplitude for one photon in the cavity."

The idea of the approach remains the same as in the case of rf control of the NV^--N coupling. For example, in order to induce the transition $(A;M_z=0) \leftrightarrow (E)$ in the NV^- center 1, we switch on the laser field $\mathcal{E}_1^{(0)}$, which is tuned to the frequency $\omega_1^{(0)}=\omega_c-E$. After performing the unitary transformation with $U=U_{\text{cavity}}U_0$, where $U_{\text{cavity}}=\exp[i\int^t dt H_{\text{cavity}}]$ and $U_0=\exp[iH_0 t]$, and then a RWA, the resulting term in the Hamiltonian will be

$$H_{\text{eff},1}^{(0)} = -g_{\text{eff},1}^{(0)}(a^\dagger\sigma_1^- + a\sigma_1^+), \quad g_{\text{eff},1}^{(0)} = \frac{g_{1z}^{(0)}\epsilon g_{1x}^{(0)}\mathcal{E}_1^{(0)}}{\omega_c}, \tag{20}$$

and similarly for the rest of the transitions. As in Ref. 27 the coupling strength is proportional to the classical field amplitude. To target only one NV^- center, we now have two strategies. One is to reproduce our earlier approach and apply a nonuniform electric field. Then, due to the Stark shift, the resonance frequency of a given NV^- center will depend on its location, and the control is realized by applying uniform optical fields at specific frequencies. [Of course, due to the nonuniform static magnetic field applied to the system, the $(A \leftrightarrow E)$ transition frequencies will already differ for different NV^- centers, but the difference is negligible.]

The other strategy is to apply laser fields locally. Given the transition wavelength of 637 nm, this may either put a lower limit on the spacing between NV^- centers or require, e.g., using evanescent modes in waveguides.

The interactions (20) can produce single-qubit rotations.[8,27] In our scheme, they can be done more easily with rf pulses. On the other hand, two-qubit gates for different NV^- centers require long-range coupling, which can be achieved through virtual excitations in the cavity. For example, if we only apply the fields $\mathcal{E}_1^{(0)}$ and $\mathcal{E}_2^{(0)}$, and eliminate the cavity modes in linear order by the Schrieffer-Wolff transformation,[28] we obtain the effective interaction

$$H_{\text{eff},12}^{(00)} = \frac{2g_{\text{eff},1}^{(0)}g_{\text{eff},2}^{(0)}}{\omega_c - E}(\sigma_1^-\sigma_2^+ + \sigma_2^-\sigma_1^+). \tag{21}$$

We will also need transitions between the ${}^3A_2$ levels $M_z=0$ (-1) and the ${}^3E$ state. They can be realized by applying another laser field with x polarization and at a corresponding resonant frequency $\approx$470 THz (λ=637 nm). The cavity degrees of freedom or other NV^- centers will not be involved.

Using Eq. (21), we can produce, e.g., an entangling transformation

$$\begin{aligned}(\alpha|M_z=0\rangle_1 + \beta|M_z=-1\rangle_1) \otimes |M_z=0\rangle_2 \\ \rightarrow (\alpha|M_z=0\rangle_1 \otimes |M_z=-1\rangle_2 \\ + \beta|M_z=-1\rangle_1 \otimes |M_z=0\rangle_2).\end{aligned} \tag{22}$$

To achieve this, we perform the following set of operations:

(1) π-pulse between $|M_z=0\rangle_1$ and $|E\rangle_1$; the result is $(\alpha|E\rangle_1+\beta|M_z=-1\rangle_1)\otimes|M_z=0\rangle_2$,

(2) π-pulse of the interaction (21), resulting in $(\alpha|M_z=0\rangle_1\otimes|E\rangle_2+\beta|M_z=-1\rangle_1\otimes|M_z=0\rangle_2)$,

(3) π-pulse between $|E\rangle_2$ and $|M_z=-1\rangle_2$; the outcome is $(\alpha|M_z=0\rangle_1\otimes|M_z=-1\rangle_2+\beta|M_z=-1\rangle_1\otimes|M_z=0\rangle_2)$, as required.

After enabling the effective NV^--NV^- coupling through the cavity, the operations on N impurities coupled to different NV^- centers can be realized in the same way as in Ref. 23.

Although the above procedure nicely demonstrates the possibility of using the cavity to perform two-qubit gates, it takes any state of the form $(\alpha|M_z=0\rangle_1+\beta|M_z=-1\rangle_1)\otimes|M_z=-1\rangle_2$ outside the computational basis. Instead, the CPHASE gate could be implemented as follows:

(1) π-pulse between $|M_z=0\rangle_1$ and $|E\rangle_1$,

(2) 2π-pulse of the interaction (21),

(3) π-pulse between $|M_z=0\rangle_1$ and $|E\rangle_1$.

An inspection of the above procedure shows that the three states $|M_z=0\rangle_1\otimes|M_z=0\rangle_2$, $|M_z=-1\rangle_1\otimes|M_z=0\rangle_2$, and $|M_z=-1\rangle_1\otimes|M_z=-1\rangle_2$ are left unchanged at the end of the procedure, whereas the state $|M_z=0\rangle_1\otimes|M_z=-1\rangle_2$ acquires a minus sign (note that we are not including here the phases accumulated as a result of single-qubit Larmor precession). This two-qubit gate, along with single-qubit rotations, forms a universal set of gates for quantum computing.

The requirements to the optical cavity are high, but not impossible. In order to resolve $\sim$1.5 GHz against the $\sim$470 THz resonant frequency, the quality factor of the cavity should be at least of order 3×10^5, while a bulk photonic crystal cavity made of diamond is expected to have a rather low quality of 3×10^4 (Ref. 29). Hopefully, it can be significantly improved using the photonic double-heterostructure approach.[30]

We could also somewhat improve the situation by adding one more step and swapping the states $|M_z=0\rangle$ and $|M_z=1\rangle$. This can be done again using the rf field $B_y(t)$ [Eq. (8)], this time with the frequency $\omega_y'=D+\kappa B_z$ (of order 4.5 GHz). This increases the difference of the states involved in the optical coupling from $\sim$1.5 to $\sim$3 GHz.

VI. CONCLUSIONS

We propose a frequency-controlled approach to coherent manipulation of spin states of NV^- centers and NV^--N complexes in diamond. It allows to address different spins through the difference in their resonance frequencies, induced by a static nonuniform magnetic field. The time-

domain manipulations are performed using uniform rf fields. Different NV^- centers and NV^--N complexes can be coupled optically through the virtual excitations in an optical cavity. Here, both frequency control with spatially uniform ac fields and with local ac fields are possible. The required cavity quality factor is high, but achievable. Our results show that small-scale quantum information processing devices based on impurity spins in diamond may be feasible in the near future.

ACKNOWLEDGMENTS

We are greatly indebted to A. Greentree and R. Hanson for very helpful remarks and suggestions, and a thorough reading of the manuscript. This work was supported in part by the NSA, LPS, ARO, JSPS CTC Program, and by the NSF. A.Z. acknowledges partial support by the NSERC Discovery Grants Program. S.A. was supported by the JSPS.

[1] E. van Oort, P. Stroomer, and M. Glasbeek, Phys. Rev. B **42**, 8605 (1990).
[2] F. Jelezko, T. Gaebel, I. Popa, M. Domhan, A. Gruber, and J. Wrachtrup, Phys. Rev. Lett. **93**, 130501 (2004).
[3] R. Hanson, O. Gywat, and D. D. Awschalom, Phys. Rev. B **74**, 161203(R) (2006).
[4] T. Gaebel, M. Domhan, I. Popa, C. Wittmann, P. Neumann, F. Jelezko, J. Rabeau, N. Stavrias, A. Greentree, S. Prawer *et al.*, Nat. Phys. **2**, 408 (2006).
[5] R. Hanson, F. M. Mendoza, R. J. Epstein, and D. D. Awschalom, Phys. Rev. Lett. **97**, 087601 (2006).
[6] L. Childress, M. V. Gurudev Dutt, J. M. Taylor, A. S. Zibrov, F. Jelezko, J. Wrachtrup, P. R. Hemmer, and M. D. Lukin, Science **314**, 281 (2006).
[7] M. D. Lukin and P. R. Hemmer, Phys. Rev. Lett. **84**, 2818 (2000).
[8] M. S. Shahriar, P. R. Hemmer, S. Lloyd, P. S. Bhatia, and A. E. Craig, Phys. Rev. A **66**, 032301 (2002).
[9] A. Greentree, P. Olivero, M. Draganski, E. Trajkov, J. Rabeau, P. Reichart, B. Gibson, S. Rubanov, S. Huntington, D. Jamieson *et al.*, J. Phys.: Condens. Matter **18**, S825 (2006).
[10] A. A. Kaplyans, V. I. Kolyshkin, and V. N. Medvedev, Sov. Phys. Solid State **12**, 1193 (1970).
[11] G. Davies and N. B. Manson, IDR, Ind. Diamond Rev. **40**, 50 (1980).
[12] D. Redman, S. Brown, and S. C. Rand, J. Opt. Soc. Am. B **9**, 768 (1992).
[13] P. Tamarat, T. Gaebel, J. Rabeau, M. Khan, A. Greentree, H. Wilson, L. Hollenberg, S. Prawer, P. Hemmer, F. Jelezko *et al.*, Phys. Rev. Lett. **97**, 083002 (2006).
[14] N. R. S. Reddy, N. B. Manson, and E. R. Krausz, J. Lumin. **38**, 46 (1987).
[15] E. van Oort, N. B. Manson, and M. Glasbeek, J. Phys. C **21**, 4385 (1988).
[16] D. A. Redman, S. Brown, R. H. Sands, and S. C. Rand, Phys. Rev. Lett. **67**, 3420 (1991).
[17] W. Smith, P. P. Sorokin, I. L. Gelles, and G. J. Lasher, Phys. Rev. **115**, 1546 (1959).
[18] L. Mandel and E. Wolf, *Optical Coherence and Quantum Optics* (Cambridge University Press, Cambridge, 1995).
[19] D. A. Lidar and J. H. Thywissen, J. Appl. Phys. **96**, 754 (2004).
[20] J. Q. You and F. Nori, Phys. Today **58**(11), 42 (2005).
[21] Y. X. Liu, L. F. Wei, J. S. Tsai, and F. Nori, Phys. Rev. Lett. **96**, 067003 (2006).
[22] S. Ashhab, J. R. Johansson, A. M. Zagoskin, and F. Nori, Phys. Rev. A **75**, 063414 (2007).
[23] A. M. Zagoskin, S. Ashhab, J. R. Johansson, and F. Nori, Phys. Rev. Lett. **97**, 077001 (2006).
[24] Y. Makhlin, G. Schon, and A. Shnirman, Rev. Mod. Phys. **73**, 357 (2001).
[25] A. Blais, A. Maassen van den Brink, and A. M. Zagoskin, Phys. Rev. Lett. **90**, 127901 (2003).
[26] A. Wallraff, D. Schuster, A. Blais, L. Frunzio, R.-S. Huang, J. Majer, S. Kumar, S. M. Girvin, and R. J. Schoelkopf, Nature (London) **431**, 162 (2004).
[27] A. Imamoglu, D. D. Awschalom, G. Burkard, D. P. DiVincenzo, D. Loss, M. Sherwin, and A. Small, Phys. Rev. Lett. **83**, 4204 (1999).
[28] J. R. Schrieffer and P. A. Wolff, Phys. Rev. **149**, 491 (1966).
[29] S. Tomljenovic-Hanic, M. J. Steel, C. Martijn de Sterke, and J. Salzman, Opt. Express **14**, 3556 (2006).
[30] B.-S. Song, S. Noda, T. Asano, and Y. Akahane, Nat. Mater. **4**, 207 (2005).